ORIGINAL PAPER

Formulation and Stability Characterization of Rutin-Loaded Oil-in-Water Emulsions

Ilyes Dammak[1] · Paulo José do Amaral Sobral[1]

Abstract In this work, formulation and characterization of oil-in-water (O/W) emulsions loaded with rutin were successfully overhead. We investigated the effect of homogenization pressure on the mean droplet size, droplet size distribution, physical stability, and rutin retention of these emulsions. O/W emulsions with a mean droplet size ($d_{3,2}$) of about 150 nm and a span of nearly the unit were formulated by microfluidization at the homogenization pressure 20–150 MPa. The O/W emulsion droplets loaded with rutin were physically stable in terms of variations of $d_{3,2}$ and span during 30 days of storage in the dark condition at 4 and 25 °C. The creaming velocity was characterized using centrifugal method showing a relative good shelf life. HPLC analysis demonstrated that 71–85% of initial rutin was retained in the fresh O/W emulsions and declined to 22–35% (w/w) for 30-day storage at 25 °C. Antioxidant activity assays confirmed that rutin-loaded emulsion participated in the antioxidant activity after encapsulation similarly to pure rutin. These results indicate that O/W emulsion systems can function as potential delivery systems to enhance bioavailability to encapsulate liposoluble antioxidant rutin for potential applications in the food industry.

Chemical compounds studied in this article:
Rutin (PubChem CID 5280805), Tween 80 (PubChem CID 5281955), Span 80 (PubChem CID 9920342)

✉ Ilyes Dammak
dammakilyes@usp.br; dammakilyes@hotmail.fr

[1] Department of Food Engineering, FZEA, University of São Paulo, Avenida Duque de Caxias Norte 225, Pirassununga, São Paulo 13635-900, Brazil

Introduction

Flavonoids, a class of secondary metabolites, have attracted increasing attention due to its pharmacological and antioxidative activities (Cao et al. 1997; Yang et al. 2015), including scavenging of free radicals, quenching of reactive oxygen species, inhibition of oxidative enzymes, and chelation of transition metals.

Rutin is a flavonoid belonging to the subclass of flavones found in various plant sources, and its antioxidant potential has been widely explored (Cushnie and Lamb 2005; Vaquero et al. 2007). Rutin was found in many plants, such as buckwheat, rhubarb, and asparagus (Yang et al. 2015). Rutin possesses a multitude of pharmacological properties. The high potential of the radical scavenging activity of rutin makes it suitable as a good antioxidant, antiinflammatory, and anticancer agent (Perk et al. 2014). With these advantages, rutin could become a highlighted nutraceutical food product.

However, rutin with a partition coefficient ($P_{octane/water}$) of 6.37 is highly hydrophobic with water solubility of 0.0639 mg/mL (Das and Kalita 2014). All of these advantages would bring many benefits if the solubility problem could be overcome. The challenge in functional or therapeutic foods is to overcome complicated problems with the solubility of functional compounds, either in water or in oil, as well as their interactions with other compounds in food matrices. The disadvantage of most flavonoids is poor solubility in water, preventing their absorption (Rothwell et al. 2005). Another important issue for flavonoid intake was raised when research evidence suggested that the bioavailability of flavonoids depends markedly on food matrices (Parada and Aguilera 2007). The interaction of flavonoids with other compounds in food matrices directly

prevented flavonoid absorption. Akhtar et al. (2014) presented solutions in which higher bioavailability of active compounds was observed when they were encapsulated in emulsion droplets.

Oil-in-water (O/W) emulsion systems have a number of applications, especially for enhancing compound solubility. High-pressure homogenization generally produces an emulsion with submicron droplets; therefore, it is one of the most frequently used methods for producing emulsion in food and pharmaceuticals (El Kinawy et al. 2012; Gao et al. 2008). Microfluidization technology is driven by high-pressure homogenization in which disruption of the droplets is caused by the intense shear, cavitation, and turbulent flow that are generated inside the fixed-geometry chamber of the microfluidizer (McClements 2004a). These disruption energies must overcome the Laplace pressures of the droplets, with smaller droplet sizes having higher pressure (McClements 2004a). The stability of the freshly formed droplets inside the microfluidizer depends on the adsorption efficiency of emulsifier molecules to the droplet surfaces (Guzey and McClements 2006).

Encapsulation of hydrophobic rutin in O/W emulsions could deliver this functional compound by preventing interaction with other compounds in food matrices and enhancing the bioavailability of rutin (Dammak et al. 2017). To the best of our knowledge, there are only few reports on rutin encapsulation in oil-in-water emulsions (Jeon et al. 1999; Šližytė et al. 2005) and in vitro antioxidant properties (Šližytė et al. 2009) and one study dealing with the physicochemical stability characterization of rutin oil-in-water emulsions (Petursson et al. 2004). Therefore, this study seeks to formulate vegetable oil-in-water emulsions loaded with rutin and to investigate their storage stability. We investigated the effect of homogenization pressure on the formulation, mean droplet size, span, and droplet size distribution of O/W emulsions loaded with rutin. We also focused on the retention of rutin in the formulated O/W emulsions. The use of O/W emulsions to encapsulate rutin could lead to precise control of the absorption and intake amount of rutin.

Material and Methods

Chemicals

Rutin hydrate (purity ≥94.0%) was purchased from Sigma-Aldrich (São Paulo, Brazil). Refined soybean oil was purchased from Cargill Agricola S.A. (São Paulo, Brazil); Tween 80, Span 80, sodium hydroxide, phenolphthalein, HPLC-grade acetonitrile, hexane, ethanol, and methanol were obtained from Labsynth (São Paulo, Brazil). 2,6-Di-tert-butyl-4-hydroxy-boxylic acid (BHT) and 1,1-diphenyl-2-picrylhydrazyl (DPPH) were purchased from Sigma-Aldrich (São Paulo, Brazil). The water used was of Milli-Q quality with conductivity at 25 °C of 0.056 μS/cm.

Measurements of Density, Viscosity, and Superficial and Interfacial Tension

The densities of the oil and aqueous phases were measured using a digital density meter DMA 4500 (Anton Paar GmbH, Graz, Austria) at 25 °C. The viscosity of the soybean oil with or without rutin and Span 80 was measured using an AMVn automatic microviscometer (Anton Paar GmbH, Graz, Austria). The interfacial tension between the two liquid phases and the superficial tension between the liquid phase and the air were measured by the Du Nouy ring method using a tensiometer (Attension Sigma 702, Espoo, Finland). All of the measurements were carried out in triplicate at 25 °C with an immersion depth of 20 mm.

Free Fatty Acid Content

The oxidation degree of the soybean oil with or without rutin and Span 80 before emulsification was evaluated by measuring the free fatty acid (FFA) content in the soybean oil according to the standard method (AOAC 2005 Method 969.33). Briefly, an oil sample was mixed with an ethanolic solution containing 2 mL of 1% (v/v) phenolphthalein in a 150-mL flask. The mixture was heated at 65 °C and titrated with 0.1 M NaOH until a faint pink color appeared and persisted. The FFA content is determined from the volume of NaOH used in titration.

Emulsion Formulation

To overcome the poor solubility of rutin in soybean oil, increasing the temperature helps to increase the solubility of rutin. We tried to solubilize rutin at the optimum condition based on the criteria of temperature tolerance at 90 °C (da Costa et al. 2002). In this study, rutin solubility in soybean oil was first determined by a dilution method. Rutin powder was initially mixed with soybean oil at a concentration of 0.5% (w/w) using a magnetic stirrer before being heated at 90 °C for 1 h. If precipitation still appeared, a lower rutin concentration was applied. In this case, the rutin concentration was decreased stepwise until a clear soybean oil solution was observed. Rutin was found to be solubilized into soybean oil at a maximum concentration of 0.1% (w/w). This rutin concentration was used for O/W emulsion formulation.

O/W emulsions were prepared using a two-step homogenization method, similar to the protocol from Tan and Nakajima (2005). Briefly, rutin was dissolved in soybean oil at a concentration of 0.1% (w/w) with heating at 90 °C for 1 h. The oil solution was cooled to room temperature; then, Span 80 was added as emulsifier at concentration of 3.75% (w/w) and well solubilized using magnetic stirrer; the resulting oil phase was used as a dispersed phase. The continuous aqueous phase contained Tween 80 as an emulsifier at a concentration of

1.25% (w/w). One hundred grams of premix with a weight ratio of dispersed phase to continuous phase of 1:9 was homogenized using a rotor-stator homogenizer (Ultra-Turrax® IKA T25, Labotechnik, Germany) at 7000 rpm for 5 min. The resulting coarse O/W emulsion was homogenized in a three pass using a microfluidizer M-110Y (Microfluidics Co., Newton, USA) with a F20 Y (75 μm) interaction chamber at a pressure of 20, 60, 100, and 150 MPa. O/W emulsions without rutin were also prepared through the procedures and conditions mentioned above. O/W emulsion samples were stored in the dark at 25 and 4 °C for 30 days.

Droplet Size Analysis

The mean droplet size of the O/W emulsions is described by the surface-weighted mean diameter ($d_{3,2}$).

The degree of the droplet size distribution is expressed by the span, defined as

$$\text{Span} = \left(d_{v,90} - d_{v,10}\right) \Big/ d_{v,50} \tag{1}$$

where $d_{v,10}$, $d_{v,50}$, and $d_{v,90}$ denote the equivalent volume diameters at 10, 50, and 90% cumulative volume.

The mean droplet size ($d_{3,2}$), span, and size distribution measurements were performed by a photon correlation spectroscopy (PCS)-based ZetaPlus particle size analyzer equipped with a Brookhaven digital correlator (Brookhaven Instrument Co., Holtsville, USA). All measurements were made at a fixed scattering angle of 90° and a temperature of 25 °C. The light source of the particle size analyzer is a solid-state laser operating at 658 nm with 30 mW power, and the signals were detected by a high-sensitivity avalanche photodiode detector.

The samples were first diluted approximately 100 times with deionized water produced using Milli-Q water system (Millipore Co., Molsheim, France) prior to each measurement to avoid multiple light scattering effects (Van Der Mark et al. 1988).

Rheological Behavior

Rheological measurements were carried out at 25 ± 0.1 °C using an AR 2000 rheometer (TA Instruments, West Sussex, UK) with cone and plate geometry (cone diameter = 16.0 mm, angle = 2°, gap = 2.0 mm). For each measurement, 2 mL of the emulsion was carefully deposited on the plateau of the rheometer. After the sample had been contacted with the cone, the exposed surface of sample was covered with a thin layer of silicone oil to prevent evaporation during the measurement. All samples were allowed to rest for 5 min after loading to allow temperature equilibration and induced stress to relax. Steady-state flow measurements were carried out in the range of 0–200 s^{-1}, and the rheological parameters (shear stress, shear rate, apparent viscosity) were obtained from the software.

Rutin Content Determination

Sample Preparation for HPLC Analysis

Samples to be used for determining the total rutin in O/W emulsions were prepared by an extraction process. Extraction samples were prepared as follows: A rutin-loaded O/W emulsion (2 mL) was mixed with 99.5% (v/v) ethanol (5 mL). Hexane (4 mL) was then mixed with the ethanolic solution. A mixture of emulsion sample and ethanol was turbid because of the presence and formation of small soybean oil particles. Hexane addition promotes solubilization of the soybean oil droplets, causing phase separation. This mixing caused the formation of two separated phases consisting of an upper clear hexane layer and a lower clear ethanolic layer. The mixed sample was subsequently centrifuged at 3000 rpm for 20 min at 25 °C. After centrifugation, the hexane layer was removed, and an eluent (5 mL) of acetonitrile/water (6:4, v/v) was added into the ethanolic layer. The mixture became turbid due to trace of soybean oil that remained in ethanolic solution. Finally, some of soybean oil droplets in ethanolic mixture were further removed by filtration through a hydrophobic PTFE membrane with a pore size of 0.2 μm. The final supernatants which composed of analytic substances, 50% ethanol, 30% acetonitrile, and 20% Milli-Q water were collected and subjected to HPLC analysis.

The amount of rutin in the continuous aqueous phase was also determined. Emulsion samples were phase-separated through ultracentrifugation (XL-70 Ultracentrifuge, Beckman Coulter) at 50,000 rpm for 35 min. After that, the aqueous solution was filtered through a hydrophilic PTFE membrane with a pore size of 0.2 mm. Finally, the liquid containing rutin-loaded micelles was subjected to HPLC analysis.

Further analysis was carried out by investigating the emulsifier effect involved in the extraction process. Oil-water mixtures loaded with rutin were prepared as follows. A soybean oil solution containing 0.1% (w/w) rutin was mixed with an aqueous solution using a vortex mixer at an oil/aqueous solution weight ratio of 1:9. The aqueous phase contained Tween 80 at concentrations of 0, 1, and 5% (w/w). After mixing, these mixtures were subjected to the extraction process, followed by a determination of the rutin amount using HPLC.

HPLC Analysis

The rutin content in the O/W emulsions was quantified by HPLC. All measurements were done in duplicate. A HPLC system was used to measure the concentration of collected samples. The system consisted of a model LC-20AD pump system (Shimadzu, Tokyo, Japan), with a Shim-Pack VP-ODS column (reverse phase C18, 4.6 cm × 250 mm, 5 μm particle size; Shimadzu, Tokyo, Japan) and a SPD-M20A photodiode array (Shimadzu, Tokyo, Japan). A mixture of methanol and water (55:45, v/v) was used as a mobile phase with a

flow rate of 1 mL/min. Rutin was detected at wavelength 356 nm with a running time of about 24 min. A 1000 ppm stock solution of rutin in methanol was prepared and appropriately diluted to give standard solutions for the calibration of the HPLC.

Antioxidant Activity

DPPH assay was carried out as described by Dammak et al. (2016). A 0.1% (w/w) stock solution of rutin in methanol and rutin-loaded O/W emulsion were prepared and appropriately diluted (250 μL) and mixed with 500 μL of ethanolic solution containing DPPH radicals (6×10^{-6} M). The mixtures were shaken vigorously and left to stand for 30 min in the dark. The absorbance was measured spectrophotometrically at 517 nm using Lambda 35 UV/Vis spectrophotometer (PerkinElmer, New York, USA). The radical scavenging activity (RSA) was calculated using the equation

$$\%\mathrm{RSA} = \left[\left(A_{\mathrm{DPPH}} - A_{\mathrm{E}} \right) \Big/ A_{\mathrm{DPPH}} \right] \times 100 \qquad (2)$$

where A_{E} is the absorbance of solution containing antioxidant and A_{DPPH} is the absorbance of DPPH solution. The synthetic antioxidant reagent butylated hydroxytoluene (BHT) was used as positive control.

Emulsion Physical Stability

The stability of rutin emulsions was measured with multisample analytical photocentrifuge (LUMiSizer, L.U.M. GmbH, Berlin, Germany), a novel instrument employing centrifugal sedimentation to accelerate the occurrence of instability phenomena such as sedimentation, flocculation, or creaming (Xu et al. 2012). In brief, this instrument allows the intensity of the transmitted near infrared light (865 nm) through the sample, to be measured as a function of time and position over the entire sample length simultaneously. The instrument simulates comprehensive emulsion separation due to applied centrifugation forces. The data are displayed as a function of the radial position, as a distance from the center of rotation (transmission profiles). The shape and progression of the transmission profiles contain information on the kinetics of the separation process and allow particle characterization, as well as evaluation of particle-particle interactions (Sobisch and Lerche 2008). The instrumental parameters used for the measurement were as follows: volume, 1.8 mL of dispersion; $2325 \times g$; $\mathrm{time_{Exp}}$, 6690 s; time interval, 30 s; temperature, 40 °C.

The creaming index represents the percentage of the initial emulsion height (HE) and the height of cream layer. The data of creaming index was displayed by the software. The higher emulsion stability was demonstrated by the larger creaming index value.

The quantification of phase separation velocity of prepared emulsions at normal gravity is of high importance and very desirable. To be able to evaluate the influence of the centrifugal force on the stability of emulsions, experiments with the same emulsion at different relative centrifugation forces (RCFs) (704, 1056, and 2325) were performed. The obtained creaming velocities for each tested RCF were plotted versus the corresponding RCF values. We obtained a linear dependency within the RCF interval applied. The extrapolation to the corresponding earth's gravity separation velocities is straightforward. The data points were fitted to a linear regression equation. Using a fixed origin, we get the general equation

$$V = A \times (\mathrm{RCF}) \qquad (3)$$

where V is the creaming velocity of the emulsion (mm/h), A is the constant value corresponding to the creaming velocity at earth's gravity (mm/h), and RCF the relative centrifugation force.

Statistical Analysis

Results were expressed as mean ± standard deviation (SD) of three measurements for the analytical determination. Statistical differences were calculated using a one-way analysis of variance (ANOVA), followed by Tukey's test. Differences were considered significant at $p < 0.05$.

Results and Discussion

Properties of the Liquid Phases

Interfacial and Superficial Tensions

Emulsion properties such as the droplet size and droplet stability usually depend on the degree of interfacial tension reduction. The effect of a hydrophobic emulsifier Span 80 addition to the oil phase (3.75% (w/w)) on the interfacial tension between the oil and water phases was investigated using Milli-Q water (Tween 80; 1.5% (w/w)). The obtained interfacial tension data are presented in Table 1.

In addition, the effect of soybean oil heating increased interfacial tension slightly but significantly ($p < 0.05$), indicating that the soybean oil hydrophobicity increased slightly after heating (Table 1). The interfacial tension in the presence of Span 80 was unaffected by the oil heating process. Span 80 considerably lowered the interfacial tension of all of the two-phase systems (around 6 mN/m).

Furthermore, we considered the effect of rutin addition to the oil phase and the interfacial tension due to the rutin chemical structure that contains hydrophobic and hydrophilic parts (Table 1). In the absence of Span 80, rutin addition increased

Table 1 Effect of soybean oil heating, rutin, and Span 80 addition to the oil phase, on measured interfacial and superficial tension, free fatty acid (FFA) content, oil density, and viscosity

	Interfacial tension (mN/m)		Superficial tension (mN/m)		Oil density (kg/m³)		Oil viscosity (mPa s)		Free fatty acid (%)	
	0% (w/w) Span 80	1% (w/w) Span 80	0% (w/w) Span 80	1% (w/w) Span 80	0% (w/w) Span 80	1% (w/w) Span 80	0% (w/w) Span 80	1% (w/w) Span 80	0% (w/w) Span 80	1% (w/w) Span 80
Unheated soybean oil	6.12 ± 0.03c	0.76 ± 0.04a	27.19 ± 0.05a	27.9 ± 0.02a	916.50 ± 1.9a	934.52 ± 1.8a	48.99 ± 1.3b	56.35 ± 1.6b	0.36 ± 0.05a	0.38 ± 0.00b
Heated soybean oil	6.33 ± 0.08b	0.80 ± 0.03a	23.66 ± 0.03c	23.84 ± 0.04b	916.48 ± 1.4a	934.01 ± 1.8a	48.83 ± 0.5b	57.23 ± 0.8b	0.47 ± 0.00a	0.49 ± 0.04a
Heated soybean oil with 0.5% (w/w) rutin	6.75 ± 0.07a	0.75 ± 0.03a	27.03 ± 0.04b	23.7 ± 0.06c	916.02 ± 1.6a	930.82 ± 1.7a	55.82 ± 0.8a	60.42 ± 1.2a	0.36 ± 0.06a	0.37 ± 0.03b

Results are expressed as mean ± standard deviation of three determinations. Means with different letters were significantly different at $p < 0.05$

the interfacial tension slightly (about 0.6 mN/m). However, in the presence of Span 80, the interfacial tension was unaffected by rutin addition, as Span 80 would have dominantly adsorbed at the oil-water interface. Thus, these results suggest that the interfacial tension was slightly affected by heating soybean oil as well as rutin addition in the absence of Span 80.

FFA Content of the Oil Phase

FFAs are always present in vegetable oils, so the FFA amount can be used to indicate the oil quality. The soybean oil used here had a low FFA content of 0.36% (Table 1). In general, heating the oil increases the FFA content due to acceleration of the oxidative deterioration of lipid. Heating soybean oil for incorporating rutin may cause lipid oxidation that could alter the properties of the emulsion (i.e., a rancid smell). The oxidation degree of the heated soybean oil with and without rutin was investigated and compared with the unheated soybean oil (Table 1). The result showed that heating soybean oil slightly increased oil oxidation in terms of FFA content (0.47% for heated soybean oil and 0.36% for unheated soybean oil). In the other hand, the heated soybean oil with rutin did not show any variations compared to the unheated soybean oil. This could be interpreted due to the high antioxidant activity of rutin, which efficiently acts even at low concentration. This is confirmed experimentally in this work. A low FFA content in the soybean oil after heating indicates that the heated soybean oil with or without rutin still maintained its original quality with slight degradation.

Effect of Microfluidization on Emulsion Properties

Mean Droplet Sizes, Span, and Droplet Size Distribution of Freshly Prepared O/W Emulsions

Figure 1a, b illustrates the effect of homogenization pressure on the $d_{3,2}$ and span of fresh O/W emulsions with and without rutin. The first step emulsification using a rotor-stator homogenizer prepared a coarse O/W emulsion with a $d_{3,2}$ of 17.3 mm and a span of 1.2. After microfluidization of the coarse O/W, the fresh O/W emulsions had the least $d_{3,2}$ of about 150 nm with span below 1, at operating pressures 100 and 150 MPa (Fig. 1a).

Increasing the homogenization pressure significantly ($p < 0.05$) reduced the $d_{3,2}$ of the O/W emulsions between 20 and 100 MPa. As for O/W emulsions loaded with rutin, their $d_{3,2}$ and span were 250 nm and 0.22 at 20 MPa and 160 nm and 0.14 at 100 MPa. The span of the fresh O/W emulsions loaded with rutin decreased gradually from 0.23 to 0.13 with increasing homogenization pressure from 20 to 150 MPa. Similar results were obtained when formulating emulsions without rutin. These results demonstrate that rutin addition hardly affected the $d_{3,2}$ and span of the O/W emulsions formulated at each homogenization pressure.
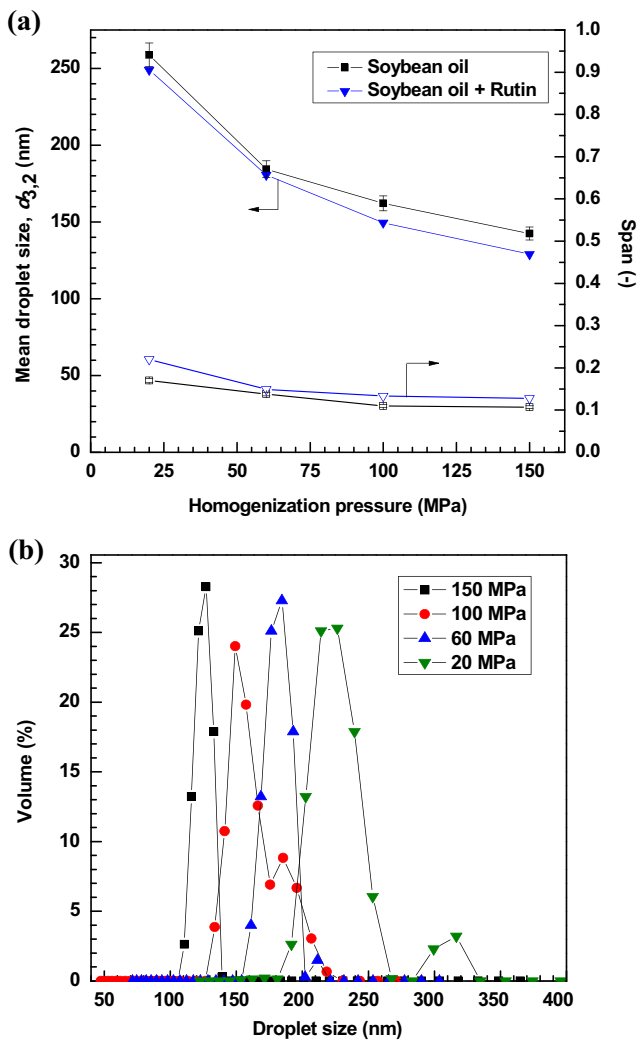
Fig. 1 **a** Effect of homogenization pressure on the mean droplet size $d_{(3,2)}$ (*closed symbols*) and span (*open symbols*). **b** Effect of homogenization pressure on droplet size distribution at 25 °C

The relationship between homogenization pressure and span can be explained by the droplet size distribution. Figure 1b plots the droplet size distributions of fresh O/W emulsions loaded with rutin. The degree of droplet size distribution was controlled by homogenization pressure. The droplet size distribution was dependent on lower homogenization pressures of 20–60 MPa but was independent of higher homogenization pressures of 60–150 MPa. The O/W emulsion formulated at a homogenization pressure of 20 MPa had a broad droplet size distribution, which may be due to an energy input that was insufficient to generate the intensive disruptive force that breaks up droplets. Increasing the homogenization pressure varied the population of droplet sizes by clearly comprising the droplet sizes into two groups.

At homogenization pressures of 60 to 150 MPa, the formulated O/W emulsions had a major droplet size distribution at about 150 nm and some droplet size distribution at about 300 nm. In this homogenization pressure range, higher

homogenization pressure enhances the population of droplet sizes at 150 nm and reduced volume frequencies in the larger droplet size range of 200–350 nm, indicating that the smallest $d_{3,2}$ and span occurred at a homogenization pressure of 150 MPa.

Effect of Tween 80 Concentration

Figure 2a illustrates the effect of the Tween 80 concentration on the formulation of O/W emulsions loaded with 0.1% rutin in the oil phase. O/W emulsions with $d_{3,2}$ of 145 to 105 nm and span of 0.17 to 0.25 were formulated using different Tween 80 concentrations (1–5% (*w/w*)) in the aqueous phase (Fig. 2a). Large droplet size was generated with Tween 80 concentration varying from 1.25 to 3.25% (*w/w*) (Fig. 2a). However, droplet size decreased to 105 and 110 nm, for higher Tween 80 concentrations from 3.5 to 5% (*w/w*) (Fig. 2a).

These results could be attributed to the interfacial tension that exceeds other major forces on a micron scale. In fact, interfacial tension plays an important role in droplet generation by microfluidization. Interfacial tensions exceeding threshold level (c.a. ~1 mN/m) are needed to stably formulate monodisperse emulsions. Karbstein and Schubert (1995) demonstrated that dynamic interfacial tension between a vegetable oil and an aqueous solution containing an emulsifier is influenced by emulsifier concentration. During W/O droplet generation in our study, dynamic interfacial tension of a newly created interface is assumed to decrease more rapidly as the Tween 80 concentration increases. These results confirm the positive role of using dual-emulsifier formulation on the physical stability of emulsion by decreasing the interfacial tension. Sessa et al. (2014) have found that optimized O/W nanoemulsion formulations caused trans-resveratrol to remain encapsulated in the oil phase during in vitro digestion. Therefore, O/W nanoemulsions, with an improved protection of the bioactive compound thanks to a dual-emulsifier formulation, can be considered as efficient delivery systems to significantly improve the bioavailability of nutraceutical and functional food ingredients.

Effect of Rutin Concentration

The effect of rutin concentration on the production of O/W emulsions by microfluidization was also investigated. Rutin content was varied from 0.01 to 0.1% (*w/w*) in the oil phase containing 3.75% (*w/w*) Span 80 and Tween 80 content of 1.25% (*w/w*) in the aqueous phase. O/W emulsions with $d_{3,2}$ of 140–147 nm and span of 0.1–0.11 were successfully formulated using different rutin concentrations in the oil phase (Fig. 2b). The $d_{3,2}$ of the O/W emulsions is not significantly affected by rutin concentration. The slight increase in droplet size may correspond toward increase in concentration of rutin. The viscosity of dispersed phase increased in the presence of rutin (Table 1), providing small area for rotor-stator homogenizer to reduce the $d_{3,2}$. As a result, a slight increase in $d_{3,2}$ of O/W emulsions was obtained
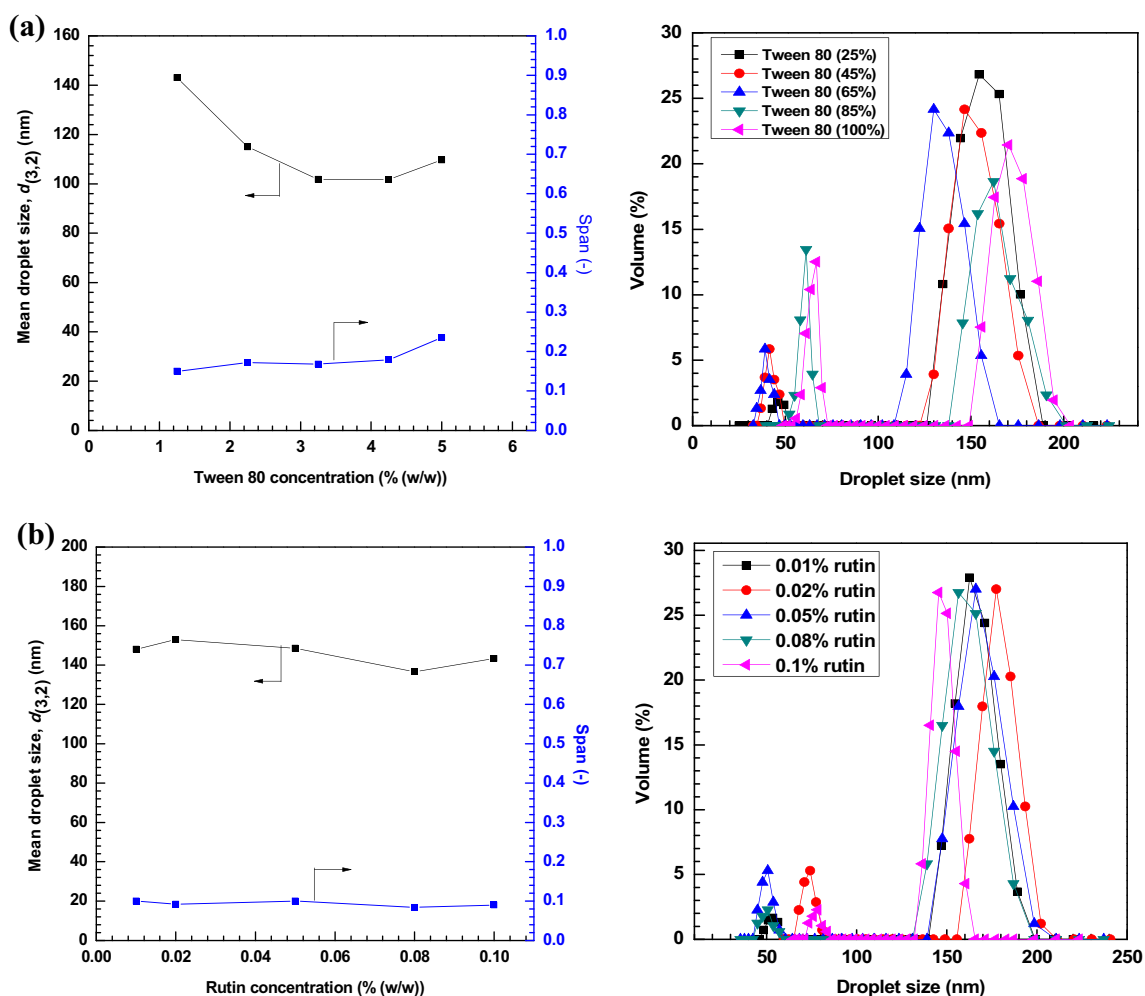
Fig. 2 **a** Effect of Tween 80 concentration and **b** rutin concentration, on mean droplet size ($d_{3,2}$), span, and droplet size distribution at 25 °C

when using a high concentration of rutin. On the other hand, the emulsifier Span 80 concentration has no effect on the $d_{3,2}$ of the W/O emulsions, which may be attributable to complete coverage of the emulsifier molecules at the interface, as clearly seen from the interfacial tension values. Smooth detachment of W/O droplets from the slot outlets was observed.

Variations in Mean Droplet Size and Droplet Size Distribution During Emulsion Storage

The emulsion stability in terms of the $d_{3,2}$ and span values of the O/W emulsions loaded with rutin was observed during 30 days of storage in the dark at 4 and 25 °C. The variations in the $d_{3,2}$ and span values during storage are illustrated in Figs. 3 and 4, respectively. During storage, the $d_{3,2}$ and span values of the resultant emulsions did not exhibit distinct changes, regardless of the homogenization pressure (Fig. 3a, b). The appearance of the O/W emulsions did not change with time. The slight increase in $d_{3,2}$ indicated that oil droplets might swell due to osmotic pressure difference. The dissolved oxygen tends to increase the

osmotic pressure over storage period, which slightly increases the $d_{3,2}$ of O/W emulsions.

Figure 3c illustrates the variation in the droplet size distribution of the rutin-loaded O/W emulsions formulated at 150 MPa during storage. The droplet size distributions showed a slight increase from 0 to 30 days. The similar relative stability of emulsion droplets was also observed in O/W emulsion at storage temperature 4 °C (Fig. 4). These results indicate that the O/W emulsions (loaded with rutin and without rutin) obtained in this study were relatively stable against coalescence and flocculation for at least 30 days. Rutin addition did not affect the trends in the $d_{3,2}$ and span values during storage at any homogenization pressure.

Qian et al. (2012) showed that the physical stability of any delivery system must also be considered before selecting it for incorporation into a particular product. β-Carotene-enriched O/W nanoemulsions have been shown to be prone to droplet aggregation at intermediate pH values (4–6), high ionic strengths (>200 mM NaCl), and elevated temperatures (>37 °C), which may limit their application in some commercial products. The information obtained from this study is

Fig. 3 **a** Effect of storage time on mean droplet size ($d_{(3,2)}$), **b** span, and **c** droplet size distribution for the prepared rutin-loaded emulsion at 100 MPa at storage temperature 25 °C
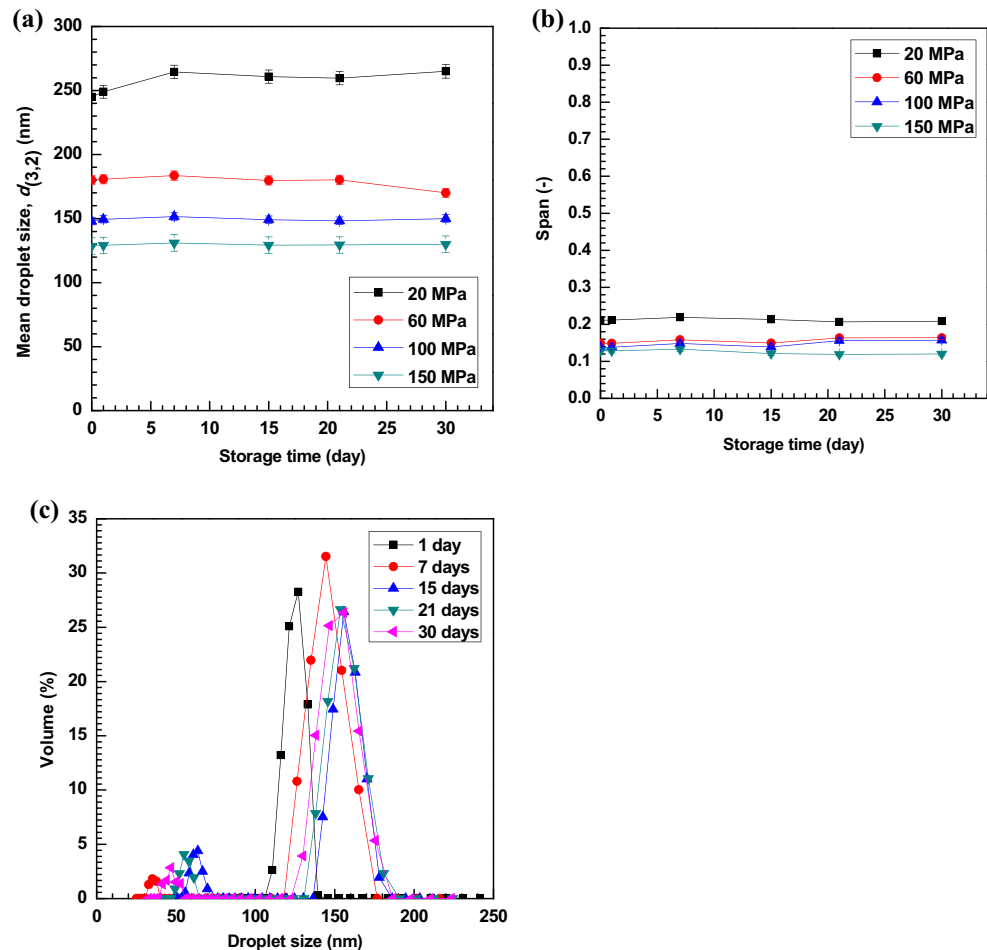
important for designing effective delivery systems to encapsulate and stabilize β-carotene for application within food, beverage, and pharmaceutical products. The use of dual-emulsifier formulation was proven to be efficient to protect considerably active compounds encapsulated. Sessa et al. (2014) reported that nanoemulsions, produced by high-pressure homogenizer, are efficient to protect trans-resveratrol from chemical degradation and to avoid reactions with oxidation and conversion to cis-resveratrol (an inactive form).

Rutin Retention

The amount of rutin present in the formulated O/W emulsions was quantitatively determined by HPLC analysis after the high-pressure homogenization formulated submicron soybean oil droplets containing rutin in the aqueous phase. The extraction fraction contained rutin, methanol, and Milli-Q water. The HPLC chromatogram represented that, within the total retention time of 12 min, the retention time of eluent exhibited a quite small peak at 2.0 min and a sharp peak of rutin at 4.3 min. As seen in Fig. 5a, higher levels of total rutin concentration were observed for fresh O/W emulsions prepared at high homogenization pressure. The total rutin concentrations

on day 0 were 71.0–85.0 μg/g of emulsion, corresponding to rutin retention of 71–85%.

During 30 days of storage, the total rutin concentration decreased for all the O/W emulsion samples (Fig. 5b). The total rutin concentrations on day 30 were 25.0–35.0 μg/g of emulsion, corresponding to rutin retention of 25–35%. The variation in the total rutin concentrations during storage is similar to the data for trans-resveratrol nanodispersions (Matos et al. 2014). The rutin retention for the O/W emulsion formulated at 20 MPa was somewhat lower than those formulated at higher homogenization pressures. We assume that this result is related to the $d_{3,2}$ of the oil droplets containing rutin (Fig. 1a). That is, higher total rutin concentrations can be obtained for rutin-loaded O/W emulsions with smaller $d_{3,2}$ values, which is opposite from the trans-resveratrol nanodispersions.

Some rutin may migrate from the oil droplets into the aqueous phase in the presence of an emulsifier, so rutin migration across the oil-water interface was investigated. Although rutin is insoluble in water, it may form small micelles stabilized by Tween 80 molecules. The rutin concentrations in the aqueous phase of the O/W emulsions on days 0 and 30 are given in Fig. 5. The rutin concentrations in the aqueous phase on day 0 were 22–40 μg/g of emulsion, corresponding to rutin retention

Fig. 4 a Effect of storage time on mean droplet size ($d_{(3,2)}$), b span, and c droplet size distribution at storage temperature 4 °C
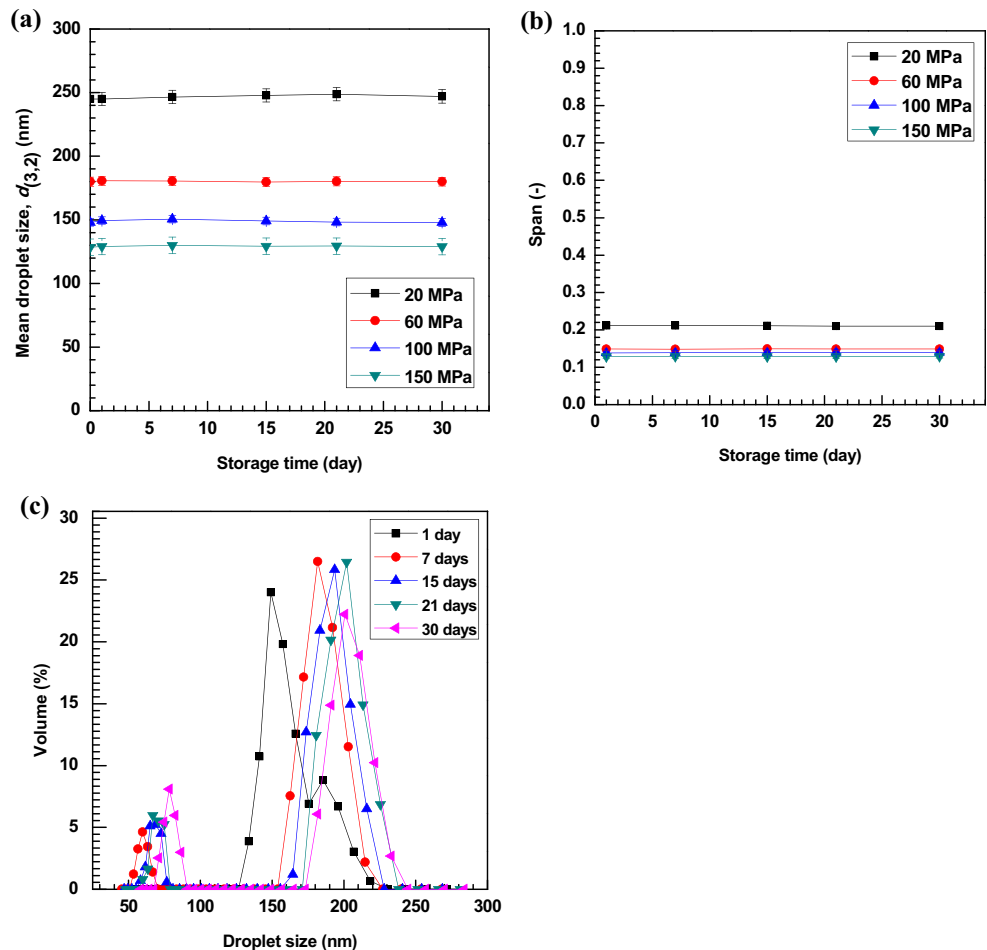
of 22–40% (w/w). As expected, small amounts of rutin were obtained in the aqueous phase, which becomes transparent after ultracentrifugation. The preceding result indicates the capability for the formation of micelles containing rutin and the encapsulation of rutin in oil droplets. During storage for 30 days, the rutin concentration in the aqueous phase decreased for all of the O/W emulsion samples. These rutin concentrations on day 30 were 8.0–12.0 μg/g of emulsion, corresponding to rutin retention of 8–12% (w/w).

Figure 1 suggests that increasing the homogenization pressure reduces the rutin concentration in the aqueous phase of O/W emulsions. The highest homogenization pressure of 150 MPa produced the O/W emulsion containing the largest rutin amount in the droplets and the smallest rutin amount in the aqueous phase, indicating that O/W emulsions with smaller droplet sizes are able to retain a larger amount of rutin in the droplets. The fresh emulsions formulated at 100 and 150 MPa gained the highest total rutin concentration of 84.0% (Fig. 5), i.e., only a small amount of the total rutin (16%) was missing.

The oxidation of rutin to further degradation products depends on several factors. Oxygen partial pressure, pH, temperature, light, and the presence of heavy metal ions are of great importance. The O/W emulsions formulated in our study were stable for more than 1 month, maintaining whitish turbidity, consistency, and flowability. The results were consistent with Sessa et al. (2014), who reported that O/W nanoemulsion successfully prepared for the encapsulation of resveratrol remained stable for 4 weeks and protected resveratrol from oxidation while maintaining its antioxidant activity.

Physical Stability of Rutin-Loaded Emulsions

Evaluation of long-term stability is often complicated by slow diffusion or chemical reaction-based destabilization processes. The result of physical stability can be quantified using an analytical centrifugation much faster and more accurately than using naked eye or analytical based on gravity demixing.

Creaming stability of the rutin emulsions were detected with multisample analytical centrifuge ($2325 \times g$, $time_{Exp.}$, 6690 s). From the transmission profile, rutin-loaded emulsions are broadly distributed. At the end of centrifugation, a cream layer of 2.2 mm is created (Fig. 6a). Calculated gravity creaming velocity showed higher shelf life for emulsion prepared with higher homogenization pressure (Fig. 6b). The higher the creaming velocity, the lower is the stability of the
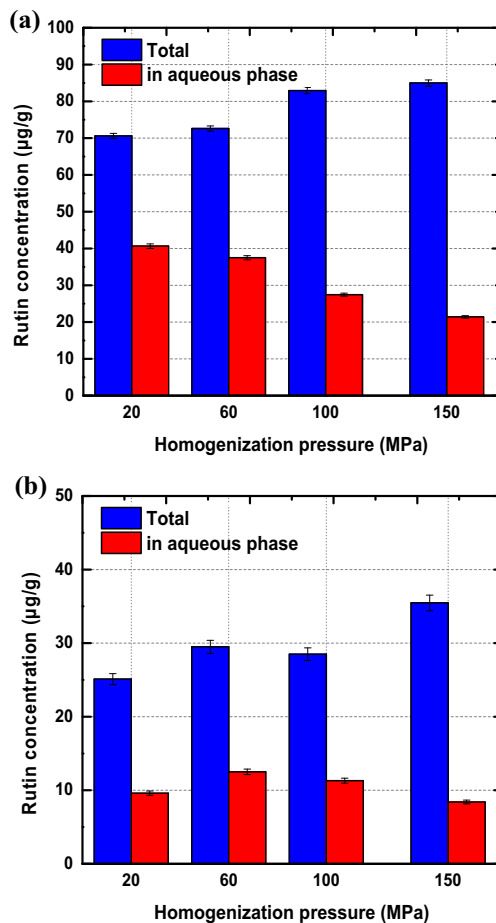
Fig. 5 Variation in rutin concentration for O/W emulsions formulated at different homogenization pressures. **a** Day 0. **b** Day 30. The *blue bar* represents the total rutin content in the emulsion. The *red bar* represents rutin content in the aqueous phase

resveratrol in nanoemulsion delivery systems enjoys different advantages in comparison with traditional delivery systems; in particular, the bioavailability of compounds encapsulated into emulsions is enhanced when emulsion droplets are of nanometric size (Salvia-Trujillo et al. 2013; Djordjevic et al. 2007).

The chemical structure of rutin might affect the physical stability of nanoemulsion, which is related to the hydrophobic and hydrophilic moieties in rutin chemical structure. Paczkowska et al. (2015) have shown that rutin binds with cyclodextrin with different proposed ways depending on the hydrophobic and hydrophilic moieties of rutin molecule. In addition, Jain et al. (2012) showed that rutin could be combined with phospholipids to form a complex more liposoluble.

Rheological Behavior of Rutin-Loaded Emulsions

The viscosity of emulsions is an important characteristic since it is related to the rate of creaming and the physical shelf life of the product (McClements 2004b). Figure 7 shows the rheological properties of rutin emulsions at 25 °C. Experimental flow curves were fitted to the Newtonian model which was the best fit model ($R^2 = 0.998$). The emulsion showed a low viscosity and nearly independent on the shear rate, with a slight decrease in the viscosity for high shear rate values. For the range of shear rates used in this study, the shear stress showed a practically linear dependence on shear rate. The viscosity decreased slightly with increasing shear rate. Shear effect is associated with the flocculation of droplets which is consistent with the above results of physical stability of the emulsion. A non-Newtonian behavior was exhibited by other protein-stabilized emulsions and was attributed to the droplet flocculation (Drakos and Kiosseoglou 2008). Flow behavior indexes of the rutin emulsions were approximately in the range of 0.99–1.0, which corresponded to Newtonian behavior.

Antioxidant Activity of Rutin-Loaded Emulsions

In order to elucidate the antioxidant properties of rutin-loaded emulsions, we applied the DPPH radical scavenging activity. DPPH is a stable free radical and accepts an electron or hydrogen to become a stable molecule. Therefore, DPPH is often used as a substrate to evaluate the antioxidant activity. DPPH radical scavenging activities of rutin and rutin emulsions are depicted in Fig. 8. All the samples tested showed a concentration dependency, and their ability to scavenge free radicals was higher with increase in concentration. For low rutin concentrations (up to 20 μg/mL), pure rutin showed a slightly higher DPPH radical scavenging activity compared to rutin-loaded emulsion and BHT. For higher rutin concentrations, the antioxidant activity of pure rutin and rutin-loaded emulsion became significantly higher than BHT. These results show that rutin have a higher free radical scavenging activity compared to the synthetic antioxidant BHT. Rutin acts as

emulsion. Sufficient stability is observed after accelerated stability test corresponding to 6 months at 25 °C.

In case of the rutin-loaded emulsions, the constant A, corresponding to earth's gravity separation velocities, was obtained by linear extrapolation (Fig. 6b). The calculated creaming velocities at earth's gravity were of 0.0034, 0.0035, 0.0039, and 0.0042 mm/h for the emulsions prepared at 150, 100, 60, and 20 MPa, respectively.

The extent of creaming was characterized by a creaming index. The creaming index provided indirect information about the extent of droplet aggregation in an emulsion. From Fig. 6c, it becomes obvious that with increasing homogenization pressure, the emulsion stability increases as well. Comparing with other applied techniques, a method for the encapsulation of resveratrol is focused on delivery systems at micrometric and nanometric scale, such as polymeric microspheres (Peng et al. 2010), biodegradable polymeric nanoparticles (Shao et al. 2009), liposomes (Narayanan et al. 2009), and O/W nanoemulsions (Sessa et al. 2014) rather than on conventional delivery forms such as tablets or capsules (Boocock et al. 2007). The encapsulation of

Fig. 6 **a** Transmission profiles for the prepared rutin-loaded emulsion at 100 MPa. **b** Creaming velocity as function of applied relative centrifugal force (RCF) for the prepared rutin-loaded emulsion at 100 MPa. **c** Change of creaming index over centrifugation time for the prepared emulsions at 20, 60, 100, and 150 MPa and 25 °C
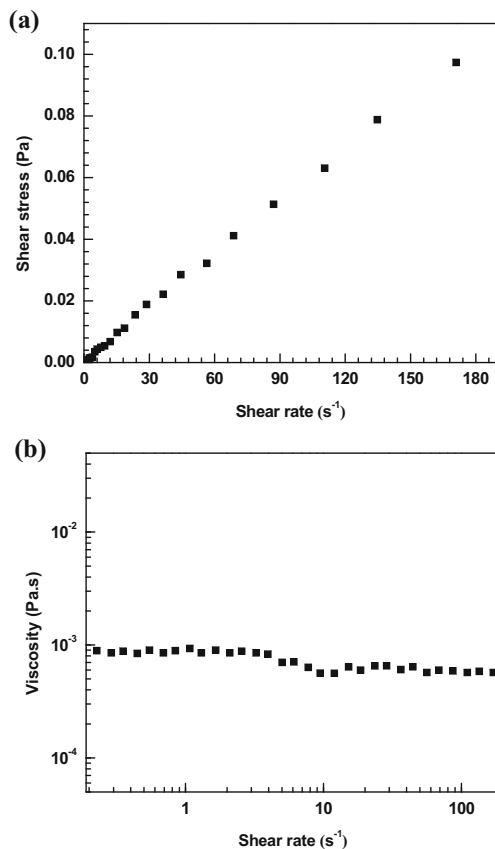
(a)

(b)
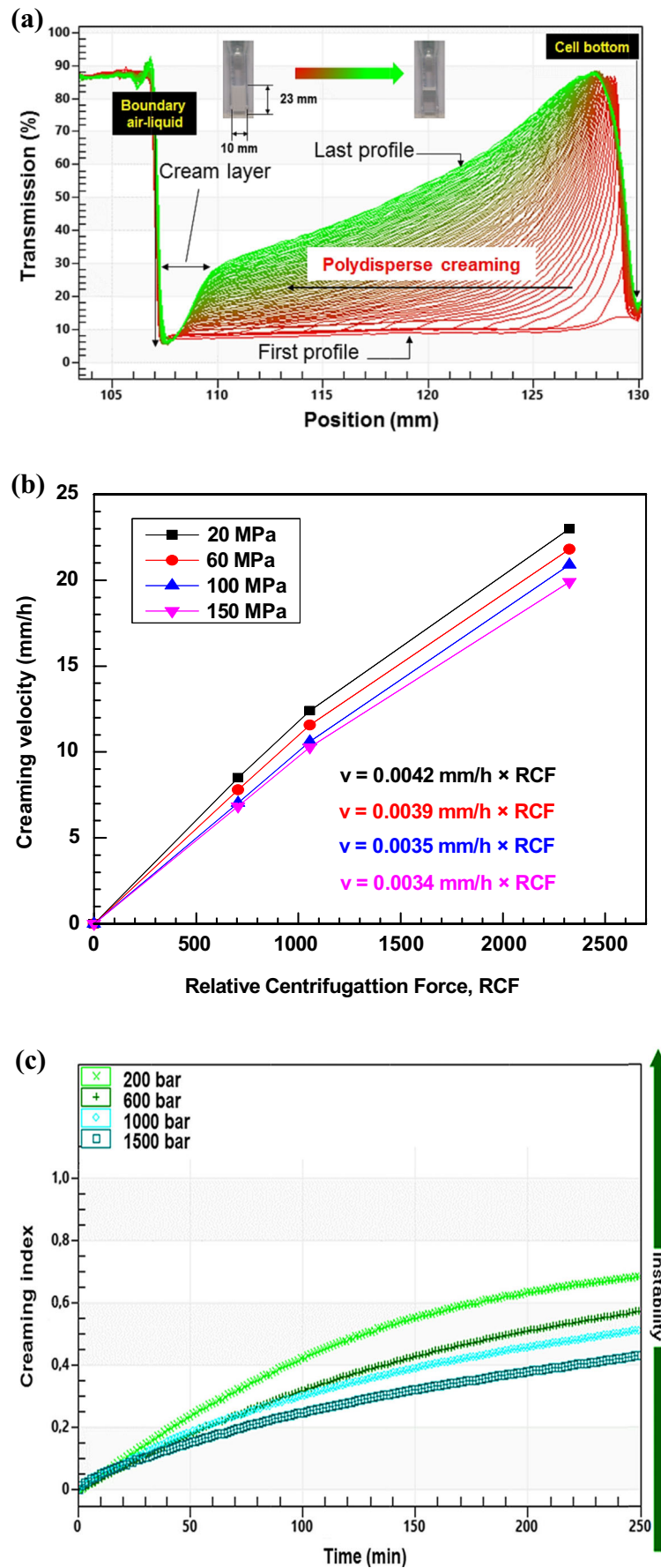
Fig. 7 Rheology of the prepared emulsion at homogenization pressure 100 MPa. **a** Measured shear stress. **b** Shear viscosity, at 25 °C

hydrogen donors and thereby converts free radicals to more stable products. Similar to our results, higher free radical scavenging activity of rutin was also reported by Yang et al. (2008). Kerdudo et al. (2014) have found that rutin was still encapsulated after 30 days loaded into multilamellar vesicles. Free rutin broke up into quercetin, while the encapsulated one
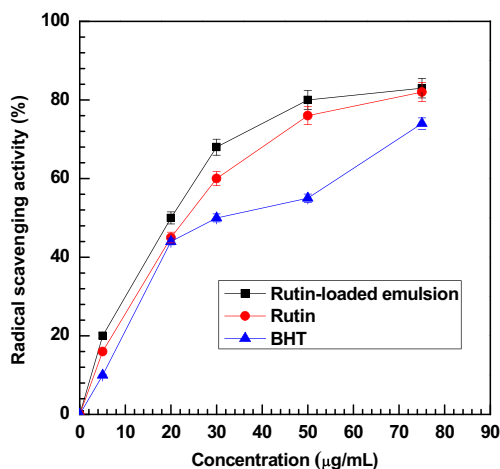

Fig. 8 DPPH radical scavenging activities of rutin, rutin-loaded emulsions and BHT

remained stable. DPPH assay confirmed that only rutin molecule participated in antioxidant activity.

These results are consistent with the results recently published by Lue et al. (2016), which revealed that rutin-loaded in O/W emulsion in high concentration (200×10^{-6} M) was more efficient than rutin esters and BHT. Interestingly, rutin had stronger antioxidative effect than BHT upon iron addition to the emulsion. Rutin may be located in closer proximity to the oxidation site than the partitioning results seem to suggest. This could at least partly explain the high protection against lipid oxidation in rutin-loaded emulsions.

Conclusions

In conclusion, our results suggest that bioactive compounds, such as rutin with low water solubility and prone to chemical and biological degradation, can be encapsulated into specially formulated food-grade emulsion-based delivery systems, to increase both their stability and bioavailability. Rutin was solubilized into refined soybean oil after heating the oil solution at 90 °C. This heating hardly affected the physical and chemical properties of rutin. Rutin-loaded O/W emulsions with mean droplet size ($d_{3,2}$) of about 150 nm were obtained after microfluidization at homogenization pressures of 100 MPa or more, and those formulated at the highest homogenization pressure (150 MPa) demonstrated the narrowest droplet size distribution in terms of span. The O/W emulsion droplets containing rutin remained physically stable with little change in their $d_{3,2}$ and span values during the entire storage period of 30 days at storage temperature of 4 and 25 °C. HPLC analysis demonstrated that rutin degradation occurred in the O/W emulsions after 30 days at 25 °C of storage and revealed the high total rutin content in the fresh O/W emulsions. The total rutin content after storage was influenced by the $d_{3,2}$ value of the rutin-loaded O/W emulsions. Calculated gravity creaming velocity showed higher shelf life for emulsion prepared with higher homogenization pressure. These results have important implications for the design and fabrication of delivery systems to encapsulate and release highly lipophilic functional ingredients.

References

AOAC official method 969.33. (2005). *Approved methods of association of official analytical chemists* (15th ed.). Washington: Association of official analytical chemists.

Akhtar, M., Murray, B. S., Afeisume, E. I., & Khew, S. H. (2014). Encapsulation of flavonoid in multiple emulsion using spinning disc reactor technology. *Food Hydrocolloids, 34*, 62–67.

Boocock, D. J., Faust, G. E., Patel, K. R., Schinas, A. M., Brown, V. A., Ducharme, M. P., Booth, T. D., Crowell, J. A., Perloff, M., Gescher, A. J., Steward, W. P., & Brenner, E. D. (2007). Phase I dose escalation pharmacokinetic study in healthy volunteers of resveratrol, a potential cancer chemopreventive agent. *Cancer Epidemiology Biomarkers & Prevention, 16*(6), 1246–1252.

Cao, G., Sofic, E., & Prior, R. L. (1997). Antioxidant and prooxidant behavior of flavonoids: structure-activity relationships. *Free Radical Biology and Medicine, 22*(5), 749–760.

Cushnie, T. T., & Lamb, A. J. (2005). Antimicrobial activity of flavonoids. *International Journal of Antimicrobial Agents, 26*(5), 343–356.

da Costa, E. M., Barbosa Filho, J. M., do Nascimento, T. G., & Macêdo, R. O. (2002). Thermal characterization of the quercetin and rutin flavonoids. *Thermochimica Acta, 392*, 79–84.

Dammak, I., Khoufi, S., & Sayadi, S. (2016). A performance comparison of olive oil mill wastewater enzymatic treatments. *Food and Bioproducts Processing, 100*, 61–71.

Dammak, I., de Carvalho, R. A., Trindade, C. S. F., Lourenço, R. V., do Amaral Sobral, P. J. (2017). Properties of active gelatin films incorporated with rutin-loaded nanoemulsions. *International Journal of Biological Macromolecules 98*, 39–49.

Das, M. K., & Kalita, B. (2014). Design and evaluation of phytophospholipid complexes (phytosomes) of rutin for transdermal application. *Journal of Applied Pharmaceutical Science, 4*(10), 51–57.

Djordjevic, D., Cercaci, L., Alamed, J., McClements, D. J., & Decker, E. A. (2007). Chemical and physical stability of citral and limonene in sodium dodecyl sulfate-chitosan and gum arabic-stabilized oil-in-water emulsions. *Journal of Agricultural and Food Chemistry, 55*(9), 3585–3591.

Drakos, A., & Kiosseoglou, V. (2008). Depletion flocculation effects in egg-based model salad dressing emulsions. *Food Hydrocolloids, 22*(2), 218–224.

El Kinawy, O. S., Petersen, S., & Ulrich, J. (2012). Technological aspects of nanoemulsion formation of low-fat foods enriched with vitamin e by high-pressure homogenization. *Chemical Engineering & Technology, 35*(5), 937–940.

Gao, L., Zhang, D., & Chen, M. (2008). Drug nanocrystals for the formulation of poorly soluble drugs and its application as a potential drug delivery system. *Journal of Nanoparticle Research, 10*(5), 845–862.

Guzey, D., & McClements, D. J. (2006). Formation, stability and properties of multilayer emulsions for application in the food industry. *Advances in Colloid and Interface Science, 128*, 227–248.

Jain, S., Dhanotiya, C., & Malviya, N. (2012). Physicochemical characterization and determination of free radical scavenging activity of rutin-phospholipid complex. *International Journal of Pharmaceutical Sciences and Research, 3*(3), 909.

Jeon, Y.-J., Byun, H.-G., & Kim, S.-K. (1999). Improvement of functional properties of cod frame protein hydrolysates using ultrafiltration membranes. *Process Biochemistry, 35*(5), 471–478.

Karbstein, H., & Schubert, H. (1995). Developments in the continuous mechanical production of oil-in-water macro-emulsions. *Chemical Engineering and Processing: Process Intensification, 34*(3), 205–211.

Kerdudo, A., Dingas, A., Fernandez, X., & Faure, C. (2014). Encapsulation of rutin and naringenin in multilamellar vesicles for optimum antioxidant activity. *Food Chemistry, 159*, 12–19.

Lue, B. M., Moltke Sørensen, A. D., Jacobsen, C., Guo, Z., & Xu, X. (2016). Antioxidant efficacies of rutin and rutin esters in bulk oil and oil-in-water emulsion. *European Journal of Lipid Science and Technology, 118*, 0000–0000.

Matos, M., Gutiérrez, G., Coca, J., & Pazos, C. (2014). Preparation of water-in-oil-in-water (W1/O/W2) double emulsions containing trans-resveratrol. *Colloids and Surfaces A: Physicochemical and Engineering Aspects, 442*, 69–79.

McClements, D. J. (2004a). *Food emulsions: principles, practices, and techniques* (pp. 254–285). Florida: CRC press.

McClements, D. J. (2004b). Protein-stabilized emulsions. *Current Opinion in Colloid and Interface Science, 9*(5), 305–313.

Narayanan, N. K., Nargi, D., Randolph, C., & Narayanan, B. A. (2009). Liposome encapsulation of curcumin and resveratrol in combination reduces prostate cancer incidence in PTEN knockout mice. *International Journal of Cancer, 125*(1), 1–8.

Paczkowska, M., Mizera, M., Piotrowska, H., Szymanowska-Powałowska, D., Lewandowska, K., Goscianska, J., & Cielecka-Piontek, J. (2015). Complex of rutin with β-cyclodextrin as potential delivery system. *PloS One, 10*(3), e0120858.

Parada, J., & Aguilera, J. (2007). Food microstructure affects the bioavailability of several nutrients. *Journal of Food Science, 72*(2), R21–R32.

Peng, H., Xiong, H., Li, J., Xie, M., Liu, Y., Bai, C., & Chen, L. (2010). Vanillin cross-linked chitosan microspheres for controlled release of resveratrol. *Food Chemistry, 121*(1), 23–28.

Perk, A. A., Shatynska-Mytsyk, I., Gerçek, Y. C., Boztaş, K., Yazgan, M., Fayyaz, S., & Farooqi, A. A. (2014). Rutin mediated targeting of signaling machinery in cancer cells. *Cancer Cell International, 14*(1), 1.

Petursson, S., Decker, E. A., & McClements, D. J. (2004). Stabilization of oil-in-water emulsions by cod protein extracts. *Journal of Agricultural and Food Chemistry, 52*(12), 3996–4001.

Qian, C., Decker, E. A., Xiao, H., & McClements, D. J. (2012). Physical and chemical stability of β-carotene-enriched nanoemulsions: influence of pH, ionic strength, temperature, and emulsifier type. *Food Chemistry, 132*(3), 1221–1229.

Rothwell, J. A., Day, A. J., & Morgan, M. R. (2005). Experimental determination of octanol-water partition coefficients of quercetin and related flavonoids. *Journal of Agricultural and Food Chemistry, 53*(11), 4355–4360.

Salvia-Trujillo, L., Qian, C., Martín-Belloso, O., & McClements, D. (2013). Influence of particle size on lipid digestion and β-carotene bioaccessibility in emulsions and nanoemulsions. *Food Chemistry, 141*(2), 1472–1480.

Sessa, M., Balestrieri, M. L., Ferrari, G., Servillo, L., Castaldo, D., D'Onofrio, N., Donsì, F., & Tsao, R. (2014). Bioavailability of encapsulated resveratrol into nanoemulsion-based delivery systems. *Food Chemistry, 147*, 42–50.

Shao, J., Li, X., Lu, X., Jiang, C., Hu, Y., Li, Q., You, Y., & Fu, Z. (2009). Enhanced growth inhibition effect of resveratrol incorporated into biodegradable nanoparticles against glioma cells is mediated by the induction of intracellular reactive oxygen species levels. *Colloids and Surfaces B: Biointerfaces, 72*(1), 40–47.

Šližytė, R., Daukšas, E., Falch, E., Storrø, I., & Rustad, T. (2005). Characteristics of protein fractions generated from hydrolysed cod (Gadus morhua) by-products. *Process Biochemistry, 40*(6), 2021–2033.

Šližytė, R., Mozuraitytė, R., Martínez-Alvarez, O., Falch, E., Fouchereau-Peron, M., & Rustad, T. (2009). Functional, bioactive and antioxidative properties of hydrolysates obtained from cod (Gadus morhua) backbones. *Process Biochemistry, 44*(6), 668–677.

Sobisch, T., & Lerche, D. (2008). Thickener performance traced by multisample analytical centrifugation. *Colloids and Surfaces A: Physicochemical and Engineering Aspects, 331*(1), 114–118.

Tan, C. P., & Nakajima, M. (2005). β-Carotene nanodispersions: preparation, characterization and stability evaluation. *Food Chemistry, 92*(4), 661–671.

Van Der Mark, M. B., van Albada, M. P., & Lagendijk, A. (1988). Light scattering in strongly scattering media: multiple scattering and weak localization. *Physical Review B, 37*(7), 3575.

Vaquero, M. R., Alberto, M., & de Nadra, M. M. (2007). Antibacterial effect of phenolic compounds from different wines. *Food Control, 18*(2), 93–101.

Xu, D., Wang, X., Jiang, J., Yuan, F., & Gao, Y. (2012). Impact of whey protein–beet pectin conjugation on the physicochemical stability of β-carotene emulsions. *Food Hydrocolloids, 28*(2), 258–266.

Yang, D., Wang, X.-Y., & Lee, J. H. (2015). Effects of flavonoids on physical and oxidative stability of soybean oil O/W emulsions. *Food Science and Biotechnology, 24*(3), 851–858.

Yang, J., Guo, J., & Yuan, J. (2008). In vitro antioxidant properties of rutin. *LWT-Food Science and Technology, 41*(6), 1060–1066.